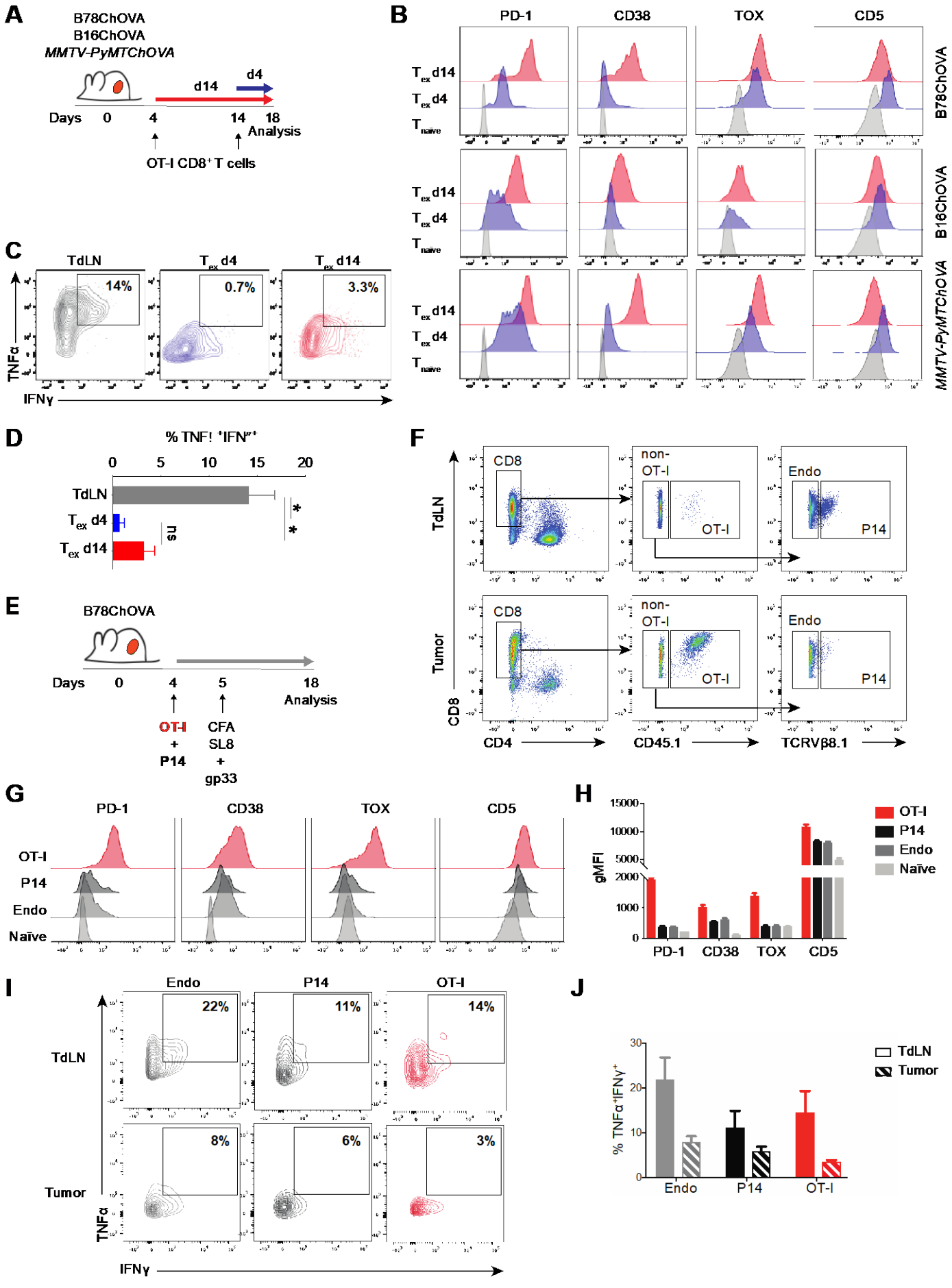
A
B78ChOVA
B16ChOVA
MMTV-PyMTChOVA
d14
d4
Days 0 4 14 18 Analysis
OT-I CD8+ T cells
B
PD-1
CD38
TOX
CD5
Tex d14
Tex d4
Tnaive
B78ChOVA
B16ChOVA
MMTV-PyMTChOVA
C
TdLN
Tex d4
Tex d14
14%
0.7%
3.3%
TNFα
IFNγ
D
% TNF+ IFNγ+
0 5 10 15 20
TdLN
Tex d4
Tex d14
ns
*
*
E
B78ChOVA
Days 0 4 5 18 Analysis
OT-I + P14
CFA SL8 + gp33
F
TdLN
Tumor
CD8
non-OT-I
OT-I
Endo
P14
CD4
CD45.1
TCRVβ8.1
G
PD-1
CD38
TOX
CD5
OT-I
P14
Endo
Naïve
H
gMFI
15000
10000
5000
2000
1000
0
PD-1
CD38
TOX
CD5
OT-I
P14
Endo
Naïve
I
Endo
P14
OT-I
TdLN
Tumor
22%
11%
14%
8%
6%
3%
TNFα
IFNγ
J
% TNFα+IFNγ+
30
20
10
0
Endo
P14
OT-I
TdLN
Tumor

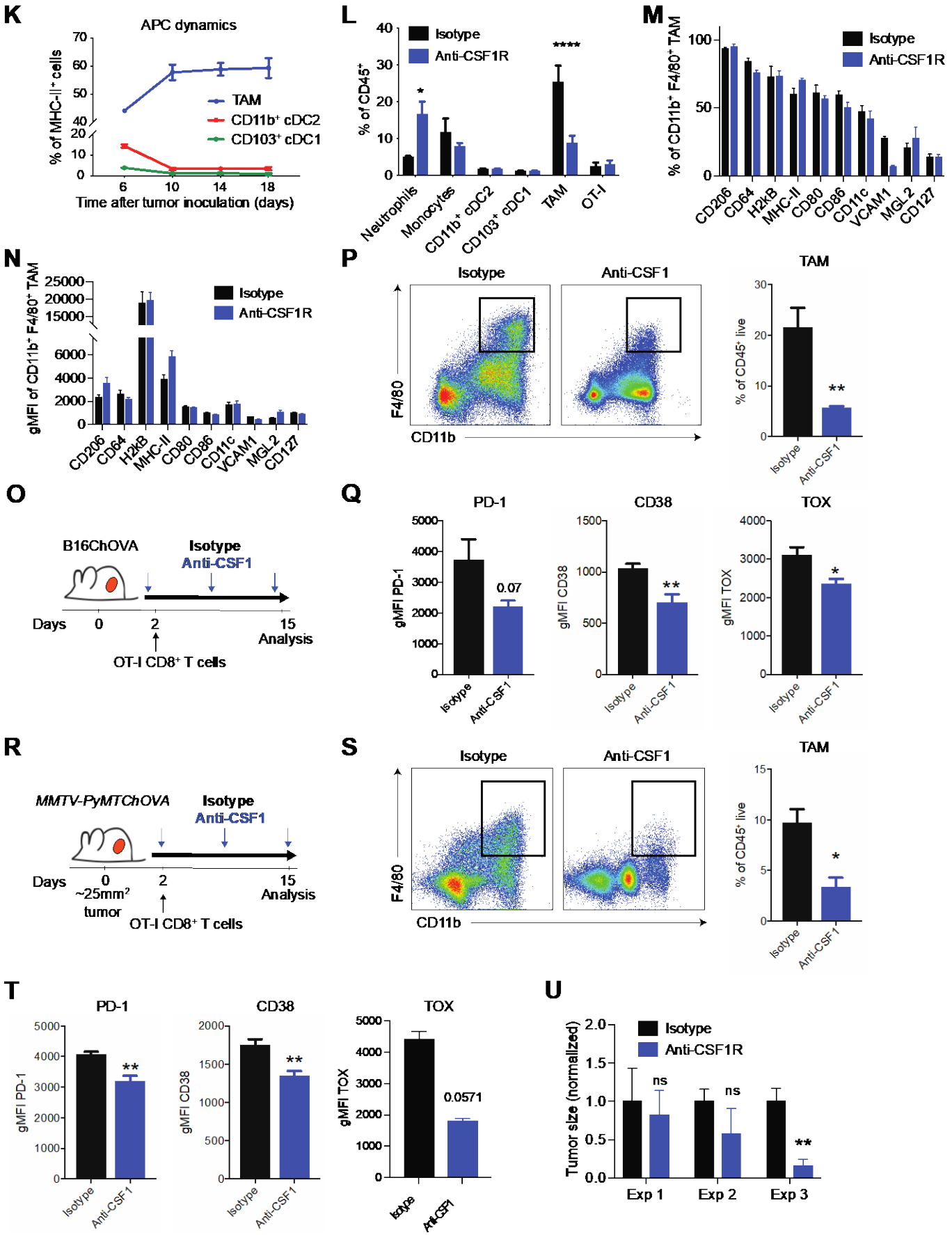

Figure S1. Onset of CD8⁺ T cell exhaustion is antigen-specific and correlates with macrophage abundance in multiple mouse cancer models (related to Figure 1). A) Experimental setup to study kinetics

of $CD8^+$ T cell exhaustion in B78ChOVA and B16ChOVA melanoma and spontaneous *MMTV-PyMTChOVA* breast cancer model. OVA-specific OT-I $CD8^+$ T cells are adoptively transferred into tumor-bearing mice 14 days (T_{ex} d14) and 4 days (T_{ex} d4) prior to sacrifice, upon which tumors are harvested for analysis of T cell phenotype at day 18. B) Representative histograms of expression of PD-1, CD38, TOX and CD5 expression on intratumoral $CD44^+$ OT-I $CD8^+$ T cells (T_{ex} d4; blue and T_{ex} d14; red), versus naïve endogenous $CD44^-$ $CD8^+$ T cells in the tumor-draining lymph node (TdLN) ($T_{naïve}$). C-D) Representative contour plots (C) and quantification (D) of $IFN\gamma^+TNF\alpha^+$ polyfunctional $CD44^+$ OT-I $CD8^+$ T cells (T_{ex} d4 and T_{ex} d14) compared to $CD44^+$ endogenous $CD8^+$ T cells in the TdLN. N=3-10 mice/group. E) Experimental setup. Mice inoculated subcutaneously with B78ChOVA melanoma cells on day 0, received adoptively transferred OT-I and p14 LCMV $CD8^+$ T cells i.v. on day 4, followed by inoculation with CFA containing SL8 + gp33 peptide s.c. on day 5. Mice were sacrificed on day 18 after tumor inoculation, and TdLN and tumors were harvested for analysis. F) Representative dot plots for the identification of endogenous (endo), and adoptively transferred $CD45.1^+$ OT-I and $TCRV\beta8.1^+$ P14 LCMV $CD8^+$ T cells in TdLN (top) and tumors (bottom) by flow cytometry. G-H) Representative histograms (G) and quantification (H) of expression of PD-1, CD38, TOX and CD5 on naïve $CD44^-$ $CD8^+$ T cells in the TdLN and on tumor-infiltrating $CD44^+$ endogenous (endo), P14 and OT-I $CD8^+$ T cells. N = 5 mice/group. I-J) Representative contour plots (I) and quantification (J) of $IFN\gamma^+TNF\alpha^+$ polyfunctional $CD44^+$ endogenous (endo), P14 and OT-I $CD8^+$ T cells in TdLN and tumor. N = 5 mice/group. Representative of two independent experiments. K) Quantification of TAM, $CD11b^+$ cDC2 and $CD103^+$ cDC1 populations represented as a fraction of $MHC\text{-}II^+$ cells in B78ChOVA tumors during tumor progression by flow cytometry. N=3 mice/time point. L) Quantification of myeloid populations in anti-CSF1R and isotype treated mice bearing B78ChOVA-melanomas as determined by flow cytometry. N=5 mice/group. M-N) Expression of phenotypic markers (as proportion (M) and gMFI (N)) on total $CD11b^+F4/80^+$ TAM in isotype and anti-CSF1R-treated B78ChOVA melanomas. N = 5-7 mice/group. O) Experimental set-up of TAM depletion in B16ChOVA-bearing mice. Weekly anti-CSF1 treatment was initiated one day prior to adoptive transfer of OT-I $CD8^+$ T cells. P) Representative dot plots and quantification of $CD11b^+$ $F4/80^+$ macrophages in isotype and anti-CSF1-treated B16ChOVA melanomas. N=5 mice/group. Q) Surface (PD-1 and CD38) and intracellular (TOX) expression on intratumoral $CD44^+$ OT-I $CD8^+$ T cells from isotype and anti-CSF1 treated B16ChOVA-bearing mice. N=5 mice/group. R) Experimental set-up of TAM depletion in spontaneous *MMTV-PyMTChOVA* breast cancer model. Weekly anti-CSF1 treatment was initiated when tumors reached ~25mm^2 in

size and one day prior to adoptive transfer of OT-I $CD8^+$ T cells. S) Representative dot plots and quantification of $CD11b^+$ $F4/80^+$ macrophages in isotype and anti-CSF1 treated mammary tumor-bearing *MMTV-PyMTChOVA* mice. N=5-6 tumors/group. T) Surface (PD-1 and CD38) and intracellular (TOX) expression on intratumoral $CD44^+$ OT-I $CD8^+$ T cells from isotype and anti-CSF1 treated mammary tumor-bearing *MMTV-PyMTChOVA* mice. N=3-6 tumors/group. U) Normalized tumor size at time of sacrifice in 3 independent experiments in B78ChOVA-bearing mice treated with isotype or anti-CSF1R. N=3-7 mice/group. All data are mean ± SEM. Statistical significance was determined using two-way ANOVA with Holm-Sidak's correction for multiple comparisons or Mann-Whitney U test. * $p < 0.05$, ** $p < 0.01$, *** $p < 0.001$.

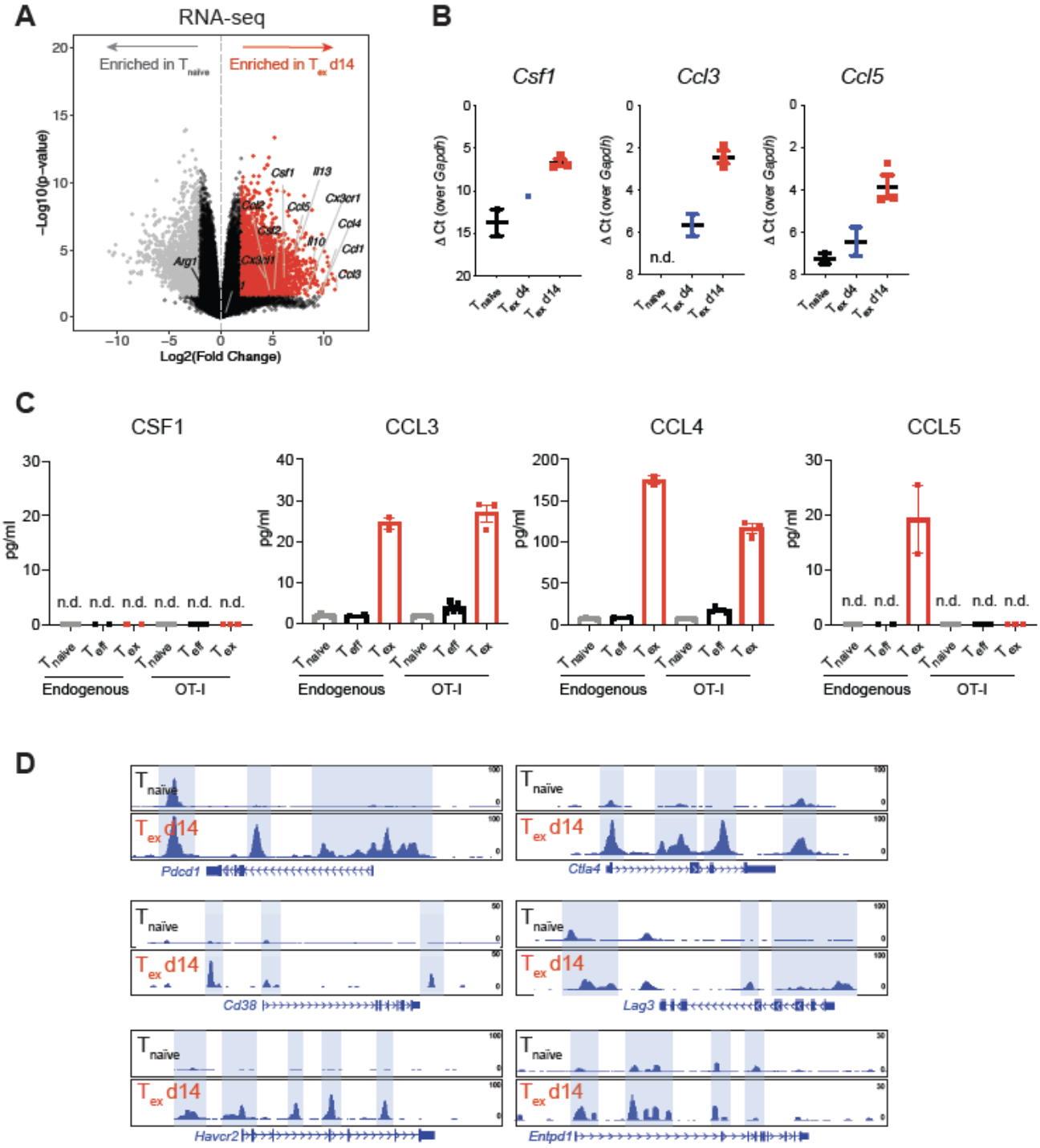

Figure S2. Transcriptional and epigenetic profiling reveals expression of myeloid-associated factors by CD8⁺ T_{ex} (related to Figure 2). A) Volcano plot showing differential gene expression in tumor-infiltrating CD44⁺ OT-I CD8⁺ T_{ex} d14 cells (red) compared to splenic CD44⁻ OT-I CD8⁺ $T_{naïve}$ cells (grey) by RNA-seq. Colored dots (grey and red) represent genes with a log2FC>2 and FDR<0.05. B) Expression of *Csf1*, *Ccl3* and *Ccl5* transcripts in an independent sample set of $T_{naïve}$, OT-I T_{ex} d4 and OT-I T_{ex} d14 T cells as determined by quantitative RT-PCR and corrected for *Gapdh.* C) Quantification of secreted protein (n.d; not detected) in supernatant of isolated

$CD44^-$ naïve, $CD44^+$ effector and $CD44^+$ exhausted endogenous and OT-I $CD8^+$ T cells after 24 hours of *ex vivo* culture as determined by ELISA (CSF1) and Cytometric Bead Array (CCL3, CCL4, CCL5). D) ATAC-seq signal tracks at the *Pdcd1*, *Cd38, Havcr2, Ctla4, Lag3* and *Entpd1* loci highlighting differential chromatin accessibility peaks in T_{ex} d14 $CD8^+$ T cells compared to splenic $CD44^-$ $T_{naïve}$ $CD8^+$ cells. All data are mean ± SEM.

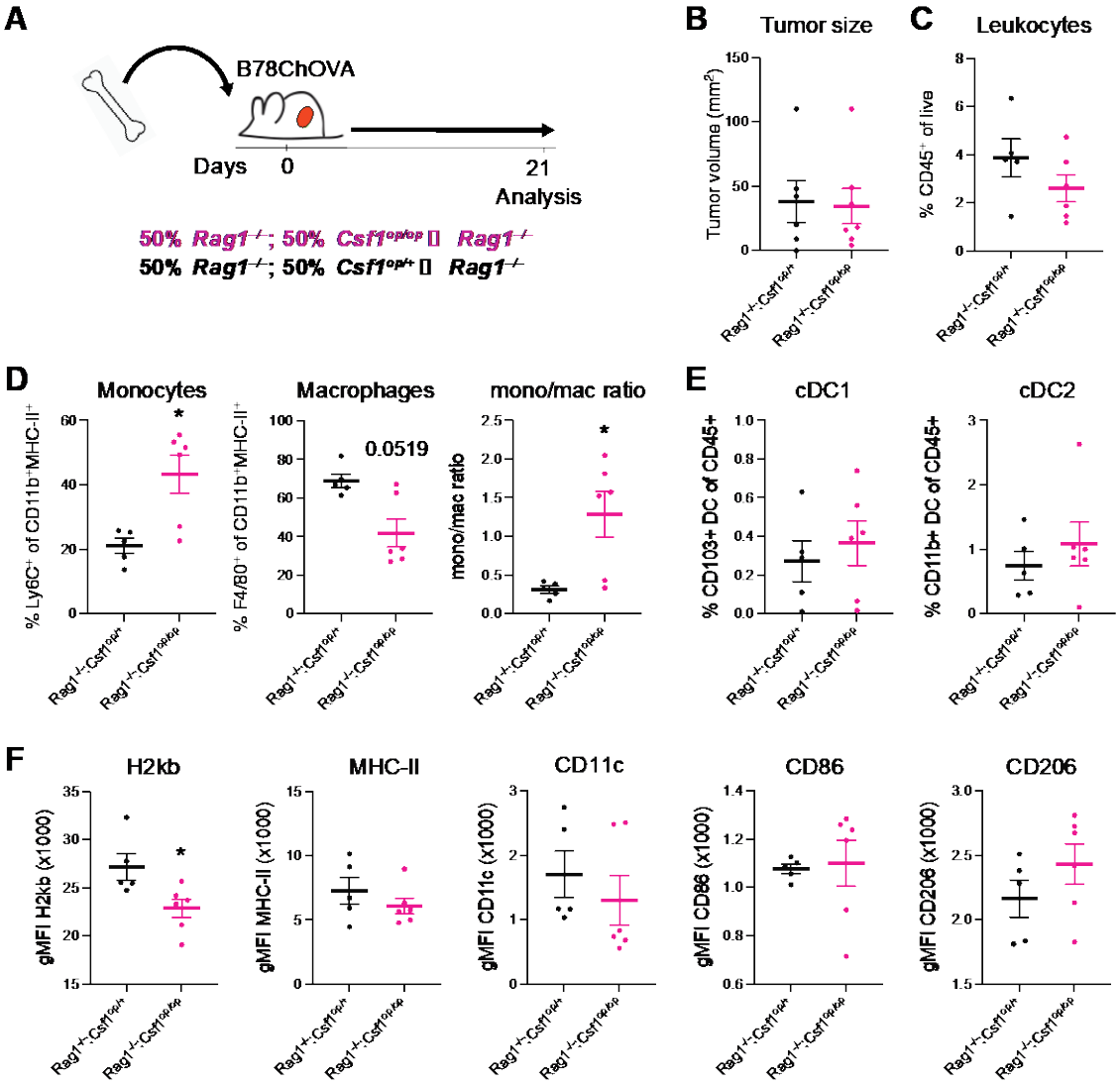

Figure S3. T cell-derived CSF1 shapes monocyte-macrophage dynamics in the TME (related to Figure 3).

A) Experimental set-up of mixed bone marrow chimeras, reconstituted with a 50:50 mixture of *Rag1*$^{-/-}$*: Csf1*$^{op/+}$ (n = 5 mice) or *Rag1*$^{-/-}$*: Csf1*$^{op/op}$ (n = 6 mice) inoculated with subcutaneous B78ChOVA melanomas 6-10 weeks after bone marrow reconstitution. 21 days later, mice were sacrificed for analysis of immune composition of tumors. B) Quantification of tumor volume (mm^2) by caliper measurements at time of sacrifice. C-E) Flow cytometric analysis of total tumor-infiltrating CD45$^+$ leukocytes (C) and (D) the proportion of Ly6C$^+$ monocytes (left), F4/80$^+$ macrophages (middle) of CD11b$^+$MHC-II$^+$ cells and monocyte/macrophage ratio (right). E) Proportion of CD103$^+$ cDC1 and CD11b$^+$ cDC2 of total CD45$^+$ cells. F) Quantification of expression of H2Kb, MHC-II, CD11c, CD86 and CD206 gated on CD11b$^+$ F4/80$^+$ macrophages (gMFI) in B78ChOVA melanomas. Representative of two independent experiments. All data are mean ± SEM. Statistical significance was determined using the Mann-Whitney U test. * $p < 0.05$.

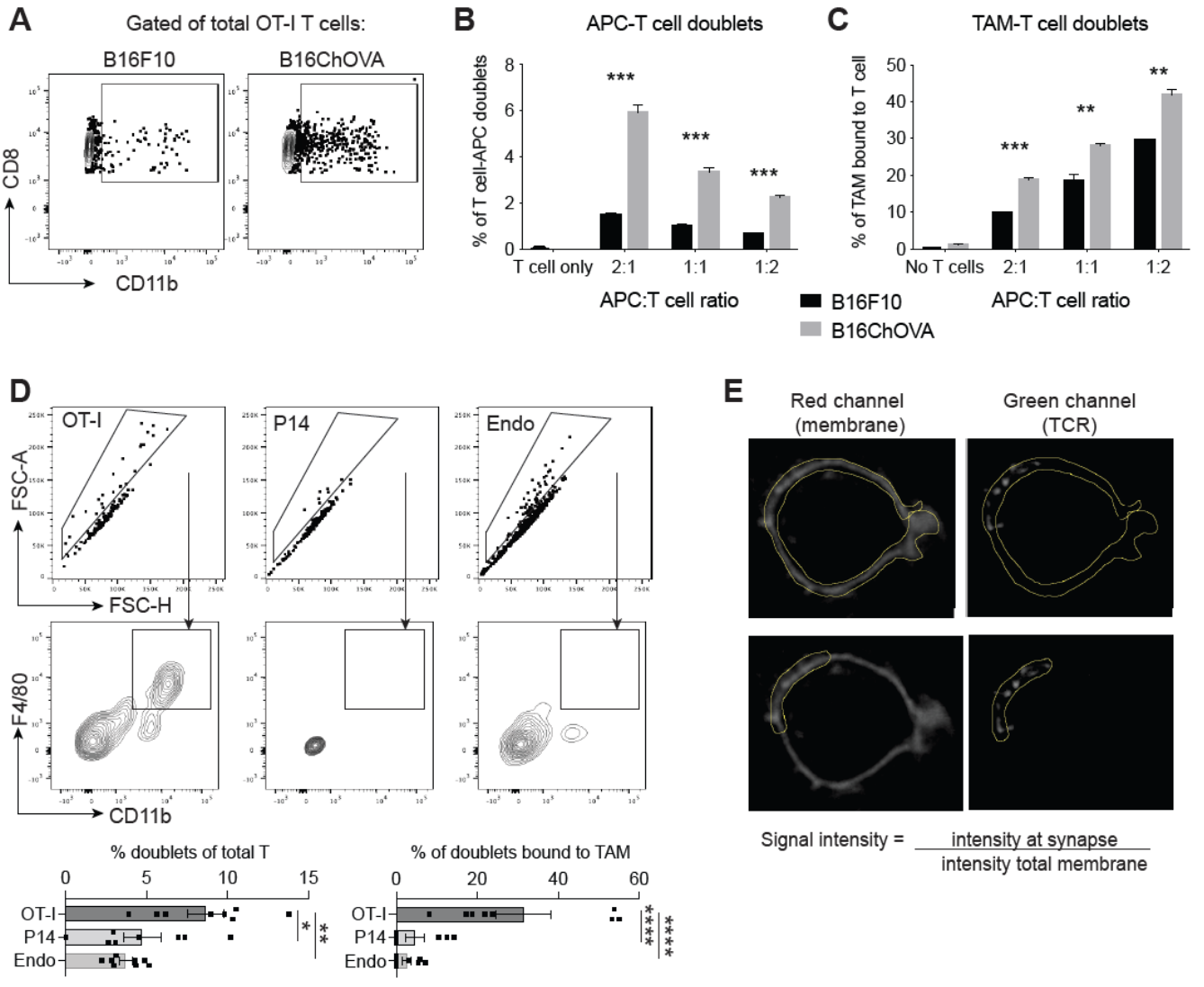

Figure S4. Synaptic TAM-CD8⁺ T cell interactions induce TCR clustering (related to Movie S1 and Figure 4). A) Representative dot plots of *ex vivo* coupling assay with CD45-enriched single cell suspensions from B16F10 or B16ChOVA melanomas co-cultured with previously activated OT-I CD8⁺ T cells gated of total T cells. B) Quantification of TAM-APC doublets of total T cells after co-culture at different APC:T cell ratios. C) Quantification of % of TAM coupled to a T cell as gated from total TAM population after co-culture at different APC:T cell ratios. Statistical significance was determined using Unpaired Student's t-test. D) Representative dot plots, contour plots and quantification of the proportion of total doublets and the proportion of those coupled to CD11b⁺F4/80⁺ TAM among OT-I, P14 and endogenous CD8⁺ T cells in B78ChOVA melanomas after enzymatic digestion. N=8 tumors in 4 mice. Statistical significance was determined using one-way ANOVA with Holm-Sidak's multiple testing correction. E) TCR clustering on the T cell membrane was quantified by manually outlining the total T cell membrane versus TAM interaction site (synapse). Signal intensity for red (membrane)

and green (TCR) channels were determined using ImageJ, and the ratio of signal intensity (synapse/total membrane) was calculated. All data are mean ± SEM. * $p < 0.05$, ** $p < 0.01$, *** $p < 0.001$, **** $p < 0.0001$.

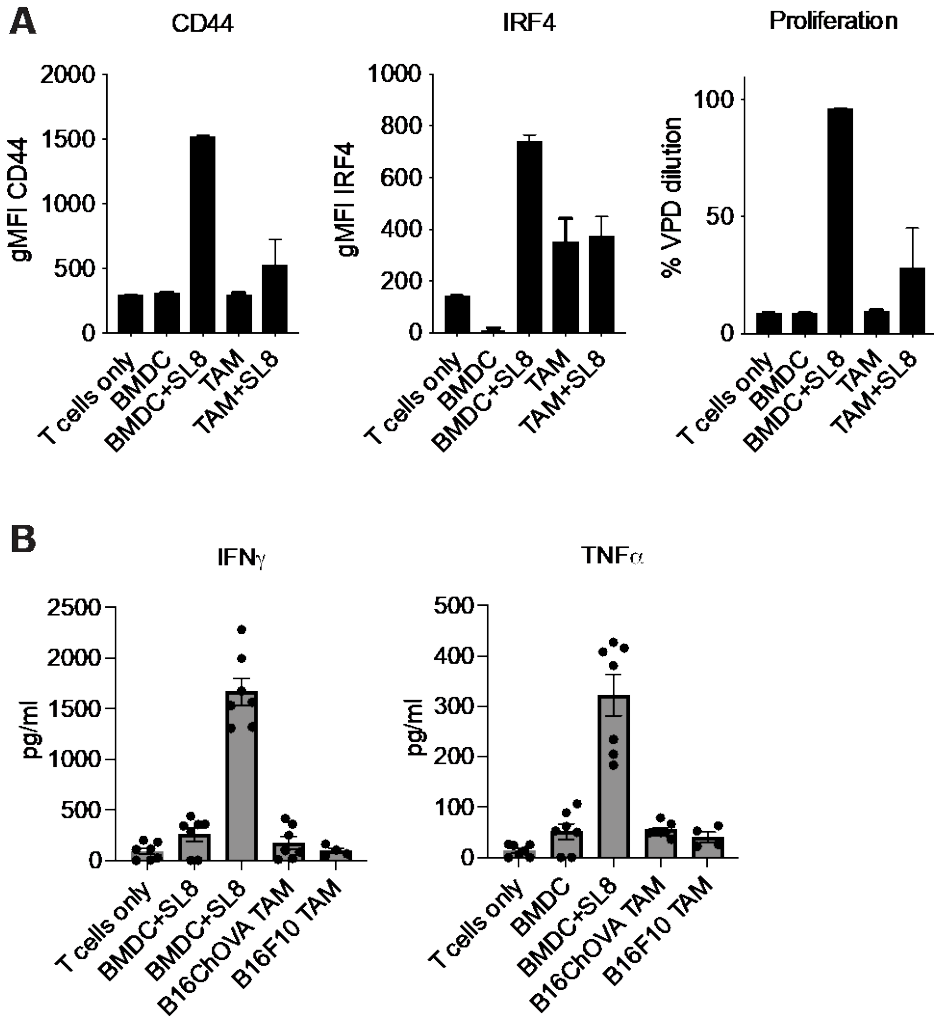

Figure S5. TAM engagement results in dysfunctional CD8⁺ T cells (related to Figure 5). A) Flow cytometric analysis of CD44, IRF4 and dilution of Violet Proliferation Dye (VPD) in previously activated CD8⁺ OT-I T cells co-cultured for 72 hours with *in vitro* generated BMDC or TAM isolated from B16ChOVA pulsed ± SL8. B) Quantification of secreted IFNγ and TNFα in supernatant after 72 hours of co-culture of previously activated CD8⁺ OT-I T cells with *in vitro* generated BMDC pulsed ± SL8 or TAM isolated from B16F10 and B16ChOVA melanomas. Pooled samples from 3 independent experiments. All data are mean ± SEM.

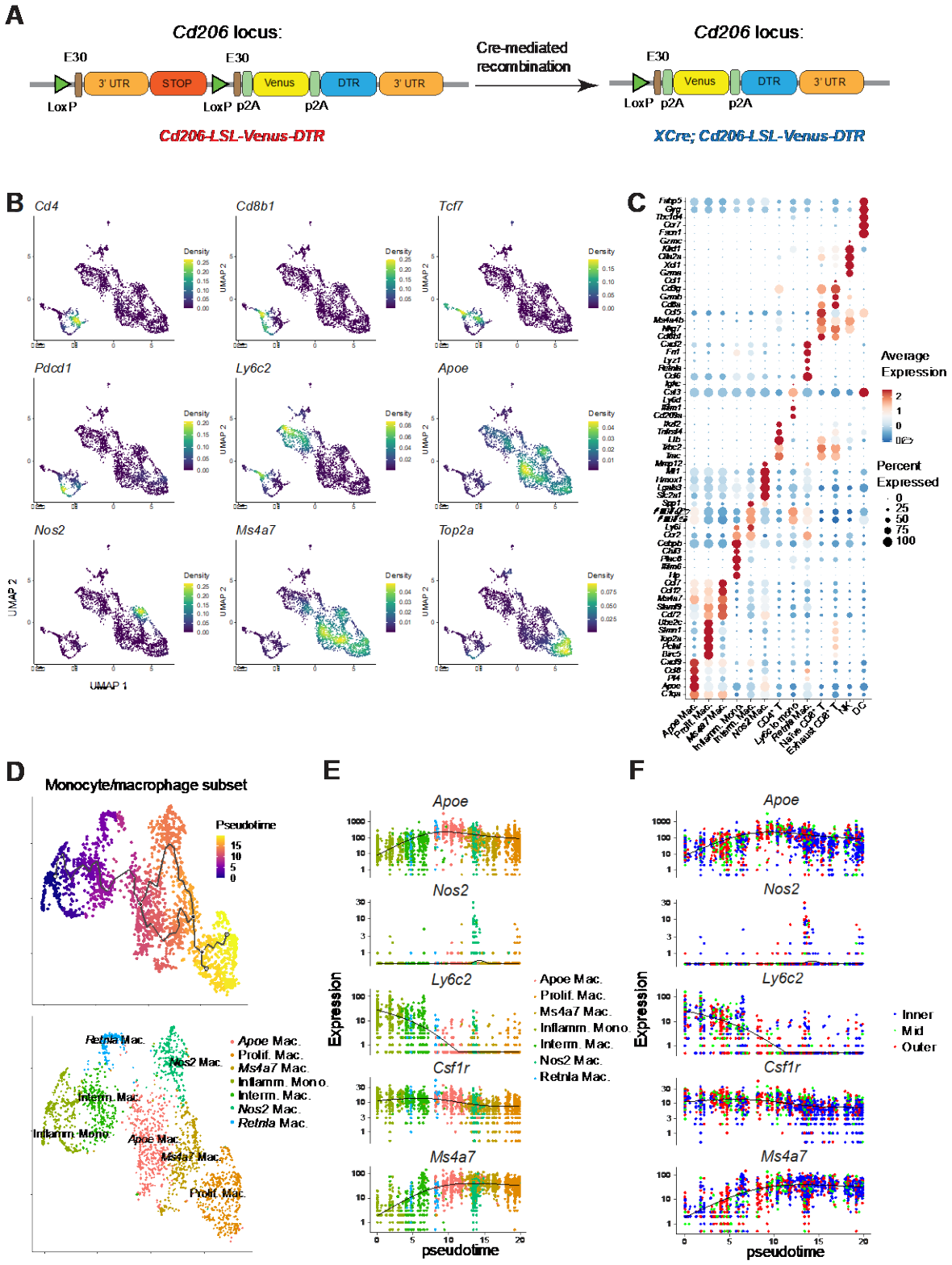

Figure S6. ZipSeq to spatially delineate TAM-T$_{ex}$ interactions in the TME (related to Figure 6). A) Schematic representation of the genetic constructs used to generate a *Cd206-LSL-Venus-DTR* reporter mouse model. Strain was crossed to *Csf1r*^{Cre} background to establish conditional deletion of the LSL cassette resulting in CD206-Venus expression specifically in myeloid cells. B) Feature plots for selected marker genes using kernel density estimates (implemented by package 'Nebulosa' (Alquicira-Hernandez and Powell, 2021)) with *Cd4*

(marking $CD4^+$ T cells), *Cd8b1* ($CD8^+$ T cells), *Tcf7* (naïve $CD8^+$ T cells), *Pdcd1* (exhausted $CD8^+$ T cells), *Ly6c2* (monocytes), *Apoe, Nos2, Ms4a7* and *Top2* (distinct macrophage subsets). C) Dot plot representation of marker gene expression (top 5 differentially expressed genes by LogFC expressed in at least 10% of cells) in annotated clusters. Dot size represents percent expression in cluster and color indicates average expression level. D) UMAP representation of monocyte/macrophage population state identity (lower) overlaid with pseudotime false-color through Monocle (upper), with *Ly6c2*^{HI} inflammatory monocyte state designated as the root state. E) Expression of genes marking distinct monocyte/macrophage populations with increasing pseudotime demonstrating that cells within our defined trajectory lose expression of *Ly6c2* while gaining expression of *Apoe* and *Ms4a7* while maintaining *Csf1r* expression. F) Pseudotime plots from E overlaid with regional localization of monocyte/macrophage subsets in B78ChOVA tumors demonstrating that *Ly6c2*^{HI} inflammatory monocytes are predominantly localized in the outer regions, while *Apoe*^{HI} and *Ms4a7*^{HI} macrophages are highly enriched in the inner regions of the TME (n = 2083 cells).

Table S1. Gene lists used in ZipSeq. (related to Figure 6).

Glycolysis (Arguello et al. 2020)	**Antigen presentation** (GO0048002)		**T cell exhaustion** (Wherry et al. 2007)				
Il7r	*Abcb9*	*Slc11a1*	*6330403K07 Rik*	*Coch*	*Id2*	*Oip5*	*Sh3bgrl*
Hmox1	*Azgp1*	*Tap1*	*Acot7*	*Cox17*	*Ifih1*	*Pawr*	*Shkbp1*
Slc2a1	*B2m*	*Tap2*	*Adam19*	*Cpsf2*	*Ifng*	*Pbx3*	*Slc29a1*
Egln3	*Bag6*	*Tapbp*	*Ahnak*	*Cpt2*	*Irf4*	*Pdcd1*	*Slc4a7*
Pkm	*Calr*	*Tapbpl*	*Alcam*	*Cryl1*	*Irf8*	*Penk*	*Smc2*
Ldha	*Cd74*	*Traf6*	*Anxa2*	*Cst7*	*Isg15*	*Perp*	*Snrpb2*
Eno1	*Clec4a2*	*Trem2*	*Art3*	*Ctla2a*	*Klra9*	*Pglyrp1*	*Snx10*
Aldoa	*Ctse*	*Unc93b1*	*Atf1*	*Ctla2b*	*Isg20*	*Plin2*	*Spock2*
Vegfa	*Ctsl*		*AW112010*	*Ctla4*	*Itga4*	*Plk4*	*Spp1*
Hif1a	*Ctss*		*Bag3*	*Cxcl10*	*Itgav*	*Plscr1*	*Stmn1*
Hk2	*Erap1*		*Bhlhe40*	*Cxcr3*	*Itgb1*	*Pon2*	*Sypl*
Pfkl	*Fcer1g*		*Bub1*	*Cyfip1*	*Itih5*	*Pqlc3*	*Tacc3*
Aldh2	*Fcgr1*		*C330007P06 Rik*	*Dock5*	*Jak3*	*Prc1*	*Tank*
Gapdh	*Fcgr2b*		*C330027C09 Rik*	*Dock7*	*Klf10*	*Prdm1*	*Tbc1d22a*
Akr1a1	*Fcgr3*		*Capzb*	*E2f8*	*Klk1*	*Ptger2*	*Tcea2*
Tpi1	*H2-Aa*		*Car2*	*Ect2*	*Klrg1*	*Ptger4*	*Tcta*
Pgam1	*H2-Ab1*		*Casp1*	*Eea1*	*Kpna2*	*Ptpn13*	*Tctn3*
Cdkn1a	*H2-D1*		*Casp3*	*Ell2*	*Lag3*	*Rbm39*	*Tfdp1*
Igf1	*H2-DMa*		*Casp4*	*Entpd1*	*Lat2*	*Rcn1*	*Tmem109*
	H2-DMb1		*Ccdc50*	*Eomes*	*Lclat1*	*Rgs16*	*Tnfrsf1a*
	H2-DMb2		*Ccl3*	*Etf1*	*Lgals1*	*Rhoq*	*Tnfrsf1b*
	H2-Eb1		*Ccl4*	*F2r*	*Lgals3*	*Pigf*	*Tnfrsf9*
	H2-K1		*Ccl5*	*Fasl*	*Litaf*	*Rnf11*	*Top2a*
	H2-M2		*Ccnb1*	*Fgl2*	*Lman2*	*Romo1*	*Tor3a*
	H2-M3		*Ccnb2*	*Fignl1*	*Lonrf1*	*Rpa2*	*Trim25*
	H2-Oa		*Ccr5*	*Fyn*	*Ly6a*	*Rpl38*	*Trim47*
	H2-Ob		*Ccr2*	*Gapdh*	*Mad2l1*	*Rps4x*	*Ttc39b*
	H2-Q4		*Ccrl2*	*Gas2*	*Mdfic*	*Rrm2*	*Tubb2a*
	H2-Q6		*Cd160*	*Gcdh*	*Mki67*	*Rsad2*	*Txn1*
	H2-Q7		*Cd200*	*Gdf3*	*Mrpl46*	*Runx2*	*Ube2t*
	H2-Q10		*Cd244*	*Gdpd5*	*Mx1*	*S100a11*	*Vamp7*
	H2-T22		*Cd7*	*Gem*	*Ndfip1*	*S100a13*	*Vamp8*
	H2-T23		*Cd84*	*Glrx*	*Nfatc1*	*S100a4*	*Vmp1*
	H2-T24		*Cd9*	*Gpd2*	*Nfil3*	*S100a6*	*Vps37a*
	Hfe		*Cdk1*	*Gpr65*	*Cbx6*	*Scin*	*Mtmr7*
	Ide		*Chek1*	*Gzma*	*Nptxr*	*Sec61g*	*Wnk1*
	Mfsd6		*Chl1*	*Gzmb*	*Nr4a2*	*Sept4*	*Zfp91*
	Mr1		*Cit*	*Gzmk*	*Nrp1*	*Serpinb6a*	
	Pikfyve		*Cks2*	*Hist3h2a*	*Nucb1*	*Serpinb9*	
	Pycard		*Clic4*	*Hmgb2*	*Nusap1*	*Sh2d2a*	